Morphogenesis and Structure of Human Teeth in Relation to Biomimetically Grown Fluorapatite−Gelatine Composites

Susanne Busch, Ulrich Schwarz, and Rüdiger Kniep*

Max-Planck-Institut für Chemische Physik fester Stoffe, Nöthnitzer Str. 40, 01187 Dresden, Germany

Received March 13, 2001. Revised Manuscript Received July 6, 2001

Biominerals are impressive composite materials because of their complex organization and perfect adaptation to the demands of living organisms. Structure and development of human teeth are compared to similar composite systems that develop in vitro under biomimetic conditions without the controlling influence of cells.

Introduction

The formation of calcified tissues in living organisms is controlled by complex processes, which are subjects of constant scientific interest. A typical feature of biominerals is usually represented by the composite nature of the materials containing inorganic and organic components. In general, the formation of these biological composite materials involve the in vivo synthesis and extracellular assembly of an organic framework, which is followed by nucleation and mineralization processes within this matrix. Special interest has been devoted to the human hard tissues bone and teeth, which are composites of apatite and proteins. Enamel is unique in the respect that the inorganic crystals are tens of micrometers in length while only a few tens of nanometers wide. These needles form typical arrangements that are highly oriented. Enamel is a tissue that, once formed and matured, can remain nearly unchanged for a lifetime because the cells that segregate the inorganic component die off when the crown formation is completed. In contrast to this, bone is a living tissue that is remodeled by being resorbed and formed again by different types of cells. The dynamic nature of continuous bone reforming hampers investigations of the involved processes to such an extent that no clear picture of the formation is obtained up to now. Thus, the structures of enamel seem to be easier to understand than those of bone. Concerning the mechanisms of the biological control over morphogenesis and structure of teeth, some aspects are known, but a complete picture of the processes involved has not emerged up to now. To simplify and reduce the enormous complexity of the problem, the role of genetic effects, chemical interactions, and cell activity in the organization of the composites has to be separated in a first step. Aiming to study the aspects of composite self-organization and the influence of growth conditions on morphogenesis and microstructure, mineralization of fluorapatite−gelatine composites was performed in vitro under biomimetic conditions. Thereby, the system apatite−gelatine is regarded as a simplified model for teeth formation because of its close chemical correspondence and remarkable analogy to structural aspects of dentine and enamel composites.

Organization of Human Teeth

Teeth are known to be the hardest calcium-phosphate-based biomineral produced by the organisms of human beings. Moreover, they show an impressive high elasticity (elastic modulus: 131 GPa [19×10^6 PSi]), although their tensile strength is rather low[1] (76 MPa [11×10^3 PSi]). The reason for this high mechanical stability is their inorganic−organic composite nature and the hierachically structured, complex organization of minute apatite crystals together with protein molecules. Human teeth are heterodont, which means that each tooth is individually shaped, in contrast to those of fish or reptiles.[2] Most morphological characteristics such as form, size, or number of roots are genetically controlled.[3] Because of the different shapes, teeth are perfectly adaptable to different tasks depending on their position in the mouth.

Every human tooth consists of a crown (corona dentis), which is visible in the mouth, and one or more roots (radix dentis), which fix the tooth in the alveoli mechanically (see Figure 1). The pulp cavity (cavitas dentis) is situated inside the tooth, containing pure organic connective tissue with incorporated nerves and vessels. Dentine-forming cells, which are called odontoblasts, are located on the surface of the pulp. The hard connective tissue of teeth can be subdivided into enamel, dentine, and tooth cement. Enamel, the outer layer of the crown, is the hardest part of the tooth (200−500 KHN Knoop scale[2]) and contains no living cells. Its density decreases from the outside to the inside from 3.00 to 2.84 g/cm^3. After the ripening process has finished, enamel consists of 95 wt % apatite, ≈3 wt % protein and lipid and 2 wt % water.[5−7] It consists of highly ordered crystal bundles, the so-called enamel prisms, which continue more or less twisted from the enamel−dentine junction to the surface of the tooth. As the prism diameter stays constant through the entire enamel, the expansion of the volume from the enamel−dentine junction toward the tooth surface can be ex-

10.1021/cm0110728 CCC: $20.00
Published on Web 09/27/2001

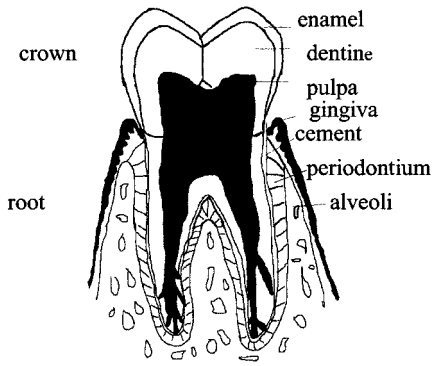

Figure 1. Schematic representation of a molar and the surrounding jaw. The tooth is fixed via the periodontium to the bone. The part that is visible in the mouth is called the crown and covered with enamel, whereas the root is situated inside the bone and the tooth.

plained by an increasing oblique orientation of the prisms.[8]

The main part of a tooth consists of dentine, which is still a living tissue. It can recover after damage as it contains appendices of dentine-forming cells (odontoblasts). In contrast to enamel, the apatite crystals are smaller and less ordered. Except for at least two proteins, which are unique in dentine,[9] the organic components are similar to bone and amount together with water up to 40 wt %. Because of its high similarity to ivory in terms of physical and optical properties, dentine is also called *substancia eburnea*. The roots are covered by tooth cementum, which is of a bone-like structure and composition. Three different cell types are involved in the development of this mineralized connective tissue and four to five different cement types are distinguished, which will not be discussed here.[10,11] Via the periodontium, which is a tough cell-rich connective tissue, the cement is connected elastically with the maxilla (upper jaw) and mandible (lower jaw), respectively (see Figure 1). The periodontium prevents resorption of the root by the organism. Replantations of lost teeth, e.g., after an accident, are only successful when this special tissue is still on the root. Cleaning before replantation leads to root resorption and rejection of the crown.[10,12]

Genesis of Human Teeth

With the development of the histological technique, the first chronological order of the human dental germ development was detected and formulated in 1794.[13] Until the beginning of the 20th century, knowledge about the processes of the odontogenesis was widely complete on a light microscopic level and the body of acquired knowledge was summarized in 1936.[14] The introduction of electron microscopy shed new light on cellular structures and the knowledge increased noticeably. However, until today many questions remain unsolved, especially those related to the storage and transport of the ionic inorganic components. The formation of dental germ starts in embryos at the end of the fourth week[15] and follows the same biological principals as the formation of successive and permanent teeth. The germs form, at the latest, a few years after birth and their development can take as long as 15 years.[10]

Teeth development covers the period from the formation of growth centers of milk teeth until the breakthrough of the permanent teeth. In human embryos, the formation of lips presumably changes the growth direction of the germ cells and, thus, induces a proliferation.[16] In the case of the dental germs, local growth limitations lead to elongations of the epithelial cells and, thus, to a proliferation and movement of the epithelium into the underlying embryonic connective tissue (mesenchyme). Thus, the early developmental stages of the dental ridge can be described as a folding of the outer oral cavity cell layer. By further folding and proliferation of the epithelium, five equidistant roundish thickenings are formed in each of the two parts of the jaw. These are called tooth buds and represent regional point shaped proliferations of the epithelium tissue and develop via the bell stage into an envelope of the future teeth. The shape is formed by the epithelial and mesenchyme cells and the resulting cavity is filled with embryonic connective tissue. The four different tooth types can be identified by their shape in the bell stage (100 days old foetus corresponding to a crown-rump-length of 70 mm). Figure 2 shows light microscopic images of histological cuts of dental germs of (a) an incisor and (b) a deciduous molar to visualize different forms of crowns that are already well-defined in this early developmental stage. These pure organic tissues represent templates for the later mineralization.

Mineralization of the Teeth

In the dental germ epithelial cells and mesenchyme cells are arranged directly opposite each other. The future enamel−dentin junction is located between the two cell types. The outer mesenchyme cells differentiate to odontoblasts and produce predentine, an organic matrix consisting mainly of collagen fibrils. This initiates the differentiation of the epithelial cells into ameloblasts. These ameloblasts are a part of the enamel organ, which consists of four different cell layers and secrete an organic matrix of complex composition that has the consistency of a gel.[17] During secretion the ameloblasts move in the direction of the later tooth surface. The secretorial ends have a typical asymmetric, noselike shape (Tomes' processes)[17] and leave a relief in the matrix that is similar to the pattern of the later formed enamel. The orientation of the long axis of the enamel prisms reflects the retraction of the ameloblasts from the enamel−dentine junction to the surface of the tooth. Moreover, the diameters of enamel prisms and ameloblasts are identical and of the order 4−6 μm. SEM images of different enamel structures in primates have been collected systematically.[18] The principle of enamel mineralization is visualized in Figure 3.

The form of the Tomes' processes undergoes an aging process that is reflected in the enamel structure. Therefore, the transverse sections of enamel prisms realize key-hole, horseshoe, or hexagonal shapes.[19] Figure 4 shows typical details of human teeth enamel as SEM images in (a) transverse and (b) parallel orientation relative to the long axis of the prisms.[20] A TEM image of an ultrathin section through an enamel prism is shown in Figure 5 to visualize the parallel orientation of the enamel crystals within the prisms.[21] As the depths of the pits are reduced with prolonged

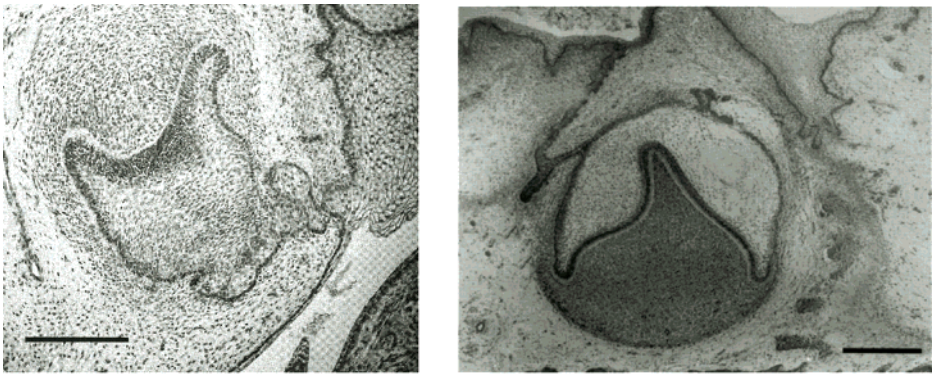

Figure 2. (a) Histological cut through the germ of a deciduous molar in the beginning bell stage. The sample was taken from a foetus with a crown-rump length of 68 mm. The morphology of the developing tooth is clearly visible. Scale bar: 125 μm. (b) Histological cut through the germ of an incisor in the bell stage. The material stems from a foetus with a crown-rump length of 95 mm. In this stage the form of the crown is fully developed. Scale bar: 250 μm. (Reproduced with friendly permission of the Quintessence Verlag[21]).

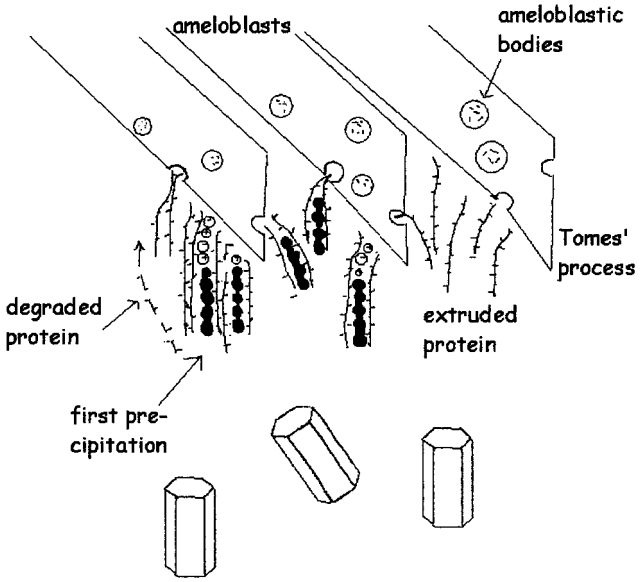

Figure 3. Schematic drawing of the principles during enamel mineralization: The ameloblasts secrete proteins and inorganic ions. Because of their retraction and the ionotropy of the gel, the protein molecules are oriented parallel. They offer nucleation sites for the first mineralization. It is assumed that an enamel crystal is the result of the coalescence of many small nucleation centers (Reproduction[17]).

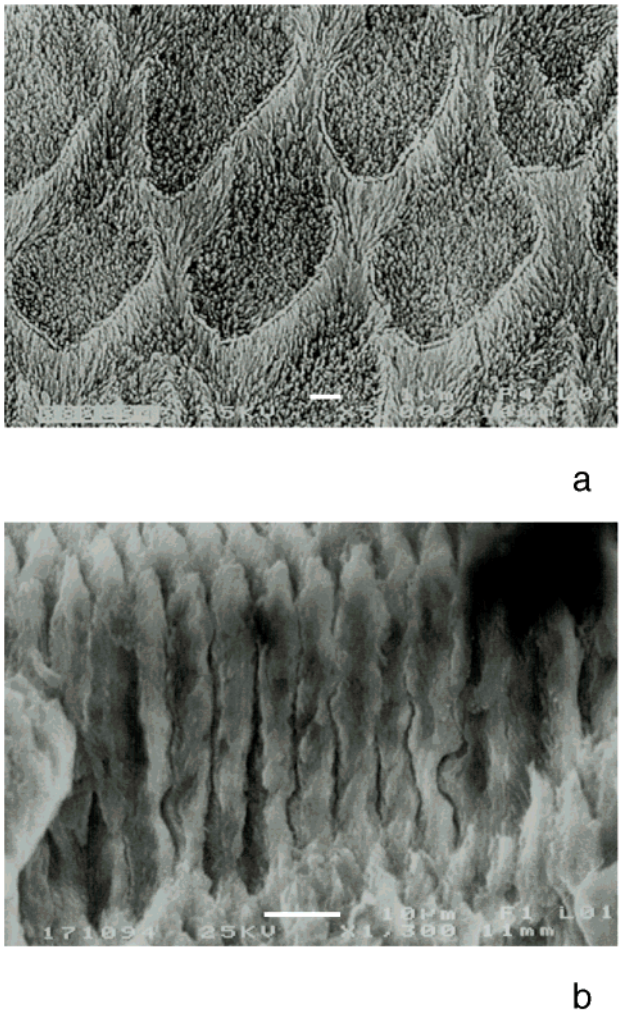

Figure 4. Scanning electron microscopy images of typical enamel prism structures. (a) Key-hole type patterns of a slice that is cut perpendicular to the long axis and etched with 50% phosphoric acid (scale bar: 1 μm) and (b) view on the long axis[20] (scale bar: 10 μm).

secretion of matrix molecules and retardation, the peripherical layers of human enamel are prism-free and consist of parallel crystals with an orientation perpendicular to the surface.[22]

During the formation period of teeth, more than 10 different proteins have been identified in samples of enamel in addition to some lipids and fatty acids[23] that make up about half of the organic matrix in enamel. Of these proteins, especially the hydrophobic amelogenin and the acidic enamelin have been investigated.

Because enamelin can only be detected after the inorganic component of enamel has been dissolved, a strong binding of this protein to the inorganic material of the enamel is assumed.[24] Amelogenin is presumably not fixed to the inorganic part of the compound, but its share of the organic enamel proteins amounts to about 90 wt %.[23] The protein assembly is hierarchically structured by building ordered nanosphere aggregates.[25] Thus, it is speculated that amelogenin serves primarily as a framework substance. Immunohystochemical investigations indicate, however, that amelogenin and

Figure 5. TEM image of an ultrathin slice of tooth enamel. Notice the regional high parallel orientation of the enamel crystals. Scale bar corresponds to 100 nm (Reproduced with friendly permission of the Quintessence Verlag[21]).

enamelin are also located in the prism cores.[26] Recent in vitro studies of the influence of amelogenin on the morphology of octacalciumphosphate showed a remarkable effect on the crystal habitus. It is assumed that the interaction of this protein with OCP crystals is stronger on (010) faces than on (100) faces as the habitus changes from a platelike shape to elongated prisms when amelogenin is present.[27] These investigations are of special importance for tooth formation because it is assumed that OCP serves as a precursor of enamel apatite.[28,29]

Enamel undergoes a ripening process that is associated with the disappearance of the ameloblasts and leads to a reduction of the protein content from 15 to 26 wt % to about 0.6−1 wt %.[5,6] Especially the unstable amelogenin is degraded and removed. The remaining cavities are first filled with water and later with growing apatite. In contrast to dentine, enamel does not contain type I collagen, but it was recently shown that type X collagen is present in the developing tooth germs[30] and contains collagenous and noncollagenous domains.[31]

The organic dentine matrix, essentially collagen in the form of an irregular network, is extruded by odontoblasts, which move opposite to the enamel-forming ameloblasts toward the pulp. In contrast to the ameloblasts, the odontoblasts leave their appendices (tubuli dentinales) in the matrix, which later will be mineralized. These tubuli reflect the movement of the cells and start at the enamel−dentine junction, continue through the entire dentine, and finally reach the surface of the pulp where the odontoblasts are aligned. A non-collagen-associated mineralization starts in the so-called matrix vesicles, which are collagen-free, membrane-surrounded entities with a diameter of 0.1 μm. Mineralization originates in these vesicles and spreads out in all directions until large compartments become calcified.[17] Early nucleation is also observed in the gap regions of the collagen fibrills. A specific dentine phosphoprotein that is secreted at the mineralization front binds to collagen fibrils in the gap region and is supposed to initiate the mineralization.[9]

With eruption of the teeth, the ameloblasts die off. Nevertheless, maturation of the enamel continues in the posteruptive phase by replacement of water and organic components by apatite.[6] This posteruptive maturation can lead to an enhanced translucency of the enamel and the tooth color turns more yellowish because the color of dentine shines through.[22]

Caries

The erupted teeth are covered with a noncellular membrane, the dental cuticle, which is made of glucoproteins of the saliva. Microorganisms populate the tooth surface and build a dense lawn called plaque.[19] It contains different proteins, calcium, phosphate, and fluoride ions and its mineralization leads to the formation of dental calculus.

It is without doubt that the consumption of sugar can initiate caries as some microorganisms are able to degrade sugar to acids that dissolve the teeth and there is experimental evidence that the presence of these bacteria is essential. In an animal experiment it was shown that rats fed with a sugar diet did not show caries when they were kept under sterile conditions. On the other hand, inoculation of special types of acid-forming streptococci produces caries lesions.[32,33] Furthermore, it was shown that acid-producing bacteria that are located in the dental plaque are able to synthesize and store polysaccharides.[19] These are degraded to organic acids, leading to a decalcification of subsurface enamel parts. Dissolution of individual enamel crystals starts in their cores and proceeds preferentially along the *c* axis.[34] Because of these lesions, the crystallites turn to be permeable for fluids without losing their shape.

The principle of subsurface demineralization is not restricted to enamel because it can be imitated in synthesized and subsequently sintered hydroxyapatite.[22,35] It is assumed that the outer crystals are dissolved in a first step. While the dissolution proceeds toward the inside, the surface remineralizes. The newly formed crystals in the outer layers are less soluble than the original mineral because the defect concentration is lower. A similar process is assumed for the early stages of enamel caries. When the lesion proceeds to the enamel−dentine junction, enamel loses its surface continuity and the hole spreads out into the softer dentine, as the microorganisms can penetrate through the dentine tubuli very quickly. Caries lesions reaching the pulp lead to a loss of tooth vitality.

The Inorganic Component of Human Teeth

The name apatite goes back to the Greek word “apate”, which means deception. The name was given because apatite was frequently confused with other minerals of rodlike hexagonal habitus, e.g., beryll and turmaline. As a biomineral, apatite is of importance as a main component of fish scales, bone, and teeth.

All three mineralized tissues of human teeth comprise composites of crystalline, partly substituted hydroxyapatite, and organic matrixes. As a model compound for the mineral component, we will use a crystalline phase of the idealized composition $Ca_5(PO_4)_3OH$ as a first approximation. Pure hydroxyapatite crystallizes either in space group $P6_3/m$ with two formula units in the unit cell[36] or in the monoclinic space group $P2_1/b$.[37,38] This nonstandard setting of the space group $P2_1/c$ (No. 14) was chosen to emphasize the similarity of the hexagonal

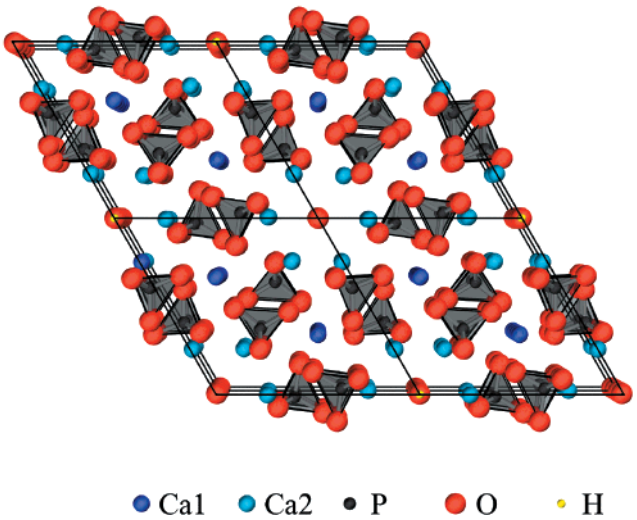

Figure 6. Hexagonal crystal structure of hydroxyapatite in a view along the *c* axis. In this presentation all OH^- ions within the same channel are oriented in the same direction; ions in neighboring channels are in opposite directions.

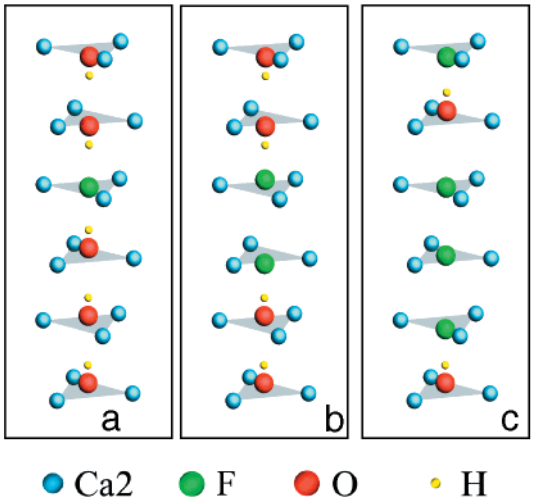

Figure 7. Different arrangements of OH^- and F^- ions in the channels of apatite. (a) In fluoride-containing hydroxyapatite the orientation of the OH^- ions can change within a channel due to the formation of OH−F hydrogen bonds. (b) With increasing fluoride content the presence of neighboring F^- ions becomes more probable and leads to repeated changes of the OH^- orientation. (c) In OH^--containing fluorapatite most OH^- ions have two F^- neighbors. The fluoride that forms the OH−F hydrogen bond is shifted out of the center of the calcium triangles.[47]

and monoclinic cell parameters. Thus, the lowering of the symmetry causes mainly a doubling of one of the hexagonal *a* axes and a slight deviation of the monoclinic angle from 120°. Figure 6 shows the hexagonal structure of hydroxyapatite. The main difference between the two forms is the arrangement of hydroxyl ions in the channels (see below). Because of composition differences of the investigated natural and synthesized samples, which will be discussed in some detail later, the published lattice parameters of abiogen hydroxyapatite show variations of the lattice parameters from $a = 942.4$ pm to $a = 943.2$ pm and for *c* in the range from 687.9 to 688.1 pm.[36,39,40]

In both modifications of hydroxyapatite, the OH^- ions are arranged along [001], that is, in columns parallel to the *c* axis. These columns pass through the centers of calcium triangles that are located on mirror planes perpendicular to the *c* axis with triangles of adjacent layers rotated by 60° with respect to each other. The oxygen atoms of the OH^- groups are displaced from the center of gravity of the calcium ions by 3 pm.[36] Because equivalent oxygen positions in the hexagonal modification have a distance of only 6 pm, which result in unreasonably short oxygen−oxygen distances, these positions are occupied at only 50%. Both different orientations of the oxygen atom are equally probable, leading to a disordered arrangement of these atoms in the crystal structure. In the monoclinic modification, all hydroxyl ions in one type of the channels are aligned in an upper direction while those of the other type point downward.[37] Channels with equally oriented hydroxyl groups are contained in layers parallel to the *a*−*c* plane. Hydroxyl groups of the adjacent layers are oriented antiparallel. Thus, the monoclinic *b* axis is doubled with respect to the *a* axes of the hexagonal unit cell and the metrical relation between the two modifications can be summarized as $a_m = a_h$, $b_m = 2a_h$, and $c_m = c_h$ with the indices m and h indicating monoclinic and hexagonal unit cell parameters, respectively.

The triangles of the calcium atoms that are arranged with a distance of 344 pm along [001] are surrounded hexagonally by a another type of calcium positions. These calcium atoms, that are labeled as type I, form tubes that are oriented parallel to [001] and, thus, to the screw axes. The type I calcium positions are coordinated by six slightly distorted phosphate tetrahedra. The phosphorus atom and two oxygen atoms are located on the same plane as the type I calcium atoms. The other two oxygen atoms are equidistant to the type II calcium atoms, which form triangles.

Replacing at least 85 mol % of the OH^- groups with chloride leads to the monoclinic chlorapatite.[41] Here, the chloride ions are displaced by 38 pm from the plane of the calcium ion triangles. When a high voltage of 5000 V/mm is applied in direction [001], the monoclinic arrangement of atoms in chlorapatite can be transformed and the atomic arrangement realizes the acentric space group $P6_3$. Under these conditions, all chloride ions are displaced from the planes in the same direction and the material becomes polar and ferroelectric.[42]

Pure fluoroapatite is hexagonal because the fluoride ions are located exactly within the plane of the calcium triangles.[43,44] Fluorapatite and hydroxyapatite form continuous solid solutions. In the case of mixed occupation of the channel positions, that is, the apatite contains OH^- as well as F^-, the fluoride ions can be displaced from the center of gravity by about 1 pm because of the formation of OH−F hydrogen bonds.[45,46] Figure 7 shows three different arrangements of the column ions in apatites, which contain both fluoride and hydroxide.[47]

In human teeth, the composition of apatite is different from the prototypes because its constituents can be replaced by a number of ions; for example, in tooth enamel more than 30 elements have been detected, and calcium is partly substituted by sodium, potassium, and other cations.[48] With regard to the anions, approximately every tenth phosphate group is replaced by hydrogen phosphate, resulting in the composition Ca_9-

$(PO_4)_{5.4}(HPO_4)_{0.6}(OH)$.[49] Additionally, 2-4 wt % of the phosphate is substituted by carbonate. Finally, part of the hydroxyl groups are replaced by fluoride, small amounts of chloride, and carbonate. Thus, carbonate replaces PO_4^{3-} groups in the framework and to a minor extent OH^- groups in the channels. Within these tubes, the CO_3^{2-} group is tilted against the 6-fold axis by about 30°.[50] The replacement of PO_4^{3-} by HPO_4^{2-} and OH^- with Cl^-, respectively, increases mainly the lattice parameter *a* of hydroxyapatite[44,51] whereas an exchange of OH^- by F^- leads to a contraction of the lattice parameter *a*.[40,44,52] Thus, substitutions of ions within the channels lead to changes that are much smaller for *c* than the alterations of *a*; for example, the lattice parameters of pure fluorapatite correspond to $a = 936.4(5)$ pm and $c = 687.9(5)$ pm whereas hydroxyapatite realizes $a = 942.2(3)$ pm and $c = 688.3(3)$.[43] Because ion replacements induce both increases and decreases of the lattice parameters, it is not possible to deduce the composition of multiply substituted apatite from the metric alone.

In enamel, a gradient of the fluoride concentration has been experimentally evidenced.[53] The decrease of the fluoride content from the outer layers toward the inner parts of enamel is attributed to an uptake of F^- from oral fluids superimposed on a baseline value due to the concentration differences ingested during tooth development.[53,54] The resulting formation of weak OH−F hydrogen bonds leads to diffusion blocking, which reduces the solubility of apatite in acids and, thus, causes a decreased probability of caries formation.[45]

Microscopic Models of Biological Apatite Formation

It is generally accepted that the activity product $[Ca^{2+}] \times [PO_4^{3-}]$ of physiological fluids is in a metastable region above the theoretical saturation level[55] of 5.5×10^{-118} ($mol^{18}\ l^{-18}$). The prevention of mineralization is the result of numerous inhibitors, for example, pyrophosphates, intermediary metabolites such as citrate, and complexing proteins.[56−59] All these molecules exhibit inhibitory effects in in vitro experiments. It is assumed that cells form the apatite−protein composite by pumping calcium and phosphate ions into a freshly extruded gel matrix. This model is supported by the experimental finding that calcium pumps (Ca-ATPase) are found in the Tomes' processes.[60] For the mineralization of cartilage it is proposed that the phosphate concentration is locally increased within the zone of calcification due to a phosphate release and due to a proteoglycan dispensation of calcium ions by ion-exchange effects.[58] This assumption is in agreement with the experimental finding that the phosphate level inside the cells is high whereas the matrix of precalcified cartilage is nearly free of phosphate.[61] However, the importance of this observation for the enamel mineralization remains to be investigated.

The retardation of the ameloblasts in combination with the influx of inorganic ions is supposed to induce a parallel orientation of the protein macromolecules due to an ionotropic effect.[5,62−64] Calcium ions are supposed to bind onto the negatively charged amino acid residues while phosphate ions bind to the positively charged amino acid residues or at the calcium ions. The mineralization of apatite starts in the direct vicinity of the ameloblasts. It was proposed that further growth of these nucleation sites leads to the formation of dotlike islands of amorphous or highly disordered apatite, which is bonded to the protein chains (see Figure 3). With proceeding growth the islands coalesce in the form of needles and the original dotlike substructure is obliterated.[64] In a next step the macromolecules are mainly decomposed and transported back to the ameloblasts whereas the needles grow in diameter and coalesce with neighboring particles. An alternative hypothesis concerning enamel formation claims that first very tiny platelike crystals form in the vicinity of the ameloblasts, which predominantly grow in the *a*−*c* plane. At the end of the embryonic stage they have a width-to thickness-ratio of about 3.9. In a second growth mechanism the flat plates fuse to mature aggregates with a width-to length ratio of 2.6.[65,66] New studies verify that initial mineralization products in the secretory stage appear as thin ribbons, which are probably octacalciumphosphate-like precursors[28,29] with spherical substructures and diameters ranging from 20 to 30 nm.[23] These ribbons are overgrown by apatite, and thus, they increase in width and thickness during the maturation stage. Enamel units as long as 100 μm but <30 nm in diameter have been isolated from developing teeth.[67] It is conceptually possible that some tooth enamel fibers are longer than 3 mm, which corresponds to the maximum thickness of the layer.[22]

As explained in the preceding parts, the factors leading to the formation of teeth are very complex and are based essentially on genetics, cell intelligence, and self-organization. At present, the precise function and the interactions of all the participating factors are not completely understood.[23] Thus, approaches aiming to imitate in vitro the formation of the biominerals dentine or enamel by maintaining the complex chemical composition of the biological system are forced to fail. Instead, it seems more promising to reduce the sophisticated biological system to only a few relevant factors.

Biomimetic Synthesis of Fluorapatite−Gelatine Composites

The basic approach of biomimetic synthesis tries to imitate the special building mechanisms of biological systems to obtain composites that are ordered from the nanometer to the mesoscopic length scale.[68] This new class of materials is interesting not only in terms of basic research and a deeper understanding of biomineralization but also with respect to expected special physical properties, for example, hardness and reduced brittleness or high porosity and, therefore, low weight in combination with high stability.[69] A first step in this field represents the examination of the influence of organic molecules on crystallization. These model systems can be nonbiological systems such as bicontinuous microemulsions,[70,71] self-assembled monolayers,[72] amphiphiles,[73] polyglyccolides,[74] and biological systems such as collagen,[75] glycosaminglycane,[76] and noncollagenous proteins.[77] Thus, it is important to study the effect of inorganic ions in the enamel matrix on the calcium phosphate mineralization. To simulate the tooth enamel formation, a cation selective membrane was used to separate calcium and phosphate ions. Addition-

ally, the influence of fluoride, magnesium, and carbonate ions on the crystal habitus of octacalciumphosphate was investigated.[78] With increasing inhibitory effect on the crystal growth ($F > Mg > CO_3^{2-}$) the crystal morphology changes from ribbonlike to flakelike particles. This result is in contrast to the observation that the morphology of early formed enamel crystals is more ribbonlike. The addition of 1 ppm fluoride leads to the formation of lamellar composites of OCP and apatite.[79] It is assumed that enamel and dentine contain OCP as well because crystals of both biominerals exibit a typical central dark line that can be observed in high-resolution electron microscopical investigations. The same dark line is observed for larger in vitro synthesized lamellar OCP crystals, which have been analyzed by transmission electron microscopical methods. Unfortunately, the size of the presumable OCP region in enamel and dentine is too small to be analyzed with X-ray diffraction methods.

A promising experiment to elucidate some basic principles of biomineralization by strongly reducing the biological active factors to pure self-organization of inorganic ions and polypeptide molecules is described in some detail.[80] The extracellular matrix for the enamel formation is simulated by a gelatine gel with a high bloom value,[81] which is the criterion for high gel tightness and, therefore, a high content of intact α-helices, which are also present in the original collagen. However, the amino acid composition of gelatine is quite different from the that of the biological organic matrix responsible for the enamel crystallization. Nevertheless, it can be assumed that gelatine can offer nucleation sites that are quite similar to the biological matrix because there is a strong chemical resemblance to collagen, which is the main part of the extracellular bone matrix.[55] In accordance with the ameloblastic secretion product, gelatine is a mixture of polypeptides with different chain lengths, which shows properties of an ionotropic gel, for example, thermoreversible gelling.[62,63] Ionotropic behavior is the requirement for orientating the organic molecules by inorganic ions that enter the experimental setup via diffusion into a gel. To avoid a fast precipitation of calcium phosphates, the buffered calcium and phosphate solutions are diffused from opposite sites into the acidified gel by means of a double-diffusion chamber.[82] The fluoride, which is necessary for fluorapatite formation, is added to the phosphate solution. The advantage of the synthesized fluorapatite in comparison to carbonate-containing hydroxyapatite, a material that is closer to natural enamel concerning chemical composition, is its higher acid resistance. Moreover, the shape of the fluorapatite units developing under the chosen biomimetic conditions are more similar to "enamel crystals" than to hydroxyapatite.[20] The fluoride content and the regular hexagonal habitus in the resulting fluorapatite aggregates closely resembles that of the enameloid of shark teeth.[24,83] The growth temperature is chosen to be 25 °C, which is rather close to the physiologic temperature of humans and low enough to prevent melting of gelatine. As a conclusion, a rather simple experimental setup enables studies of the development of a hierarchically ordered composite structure consisting of fluorapatite−gelatine nanoparticles.

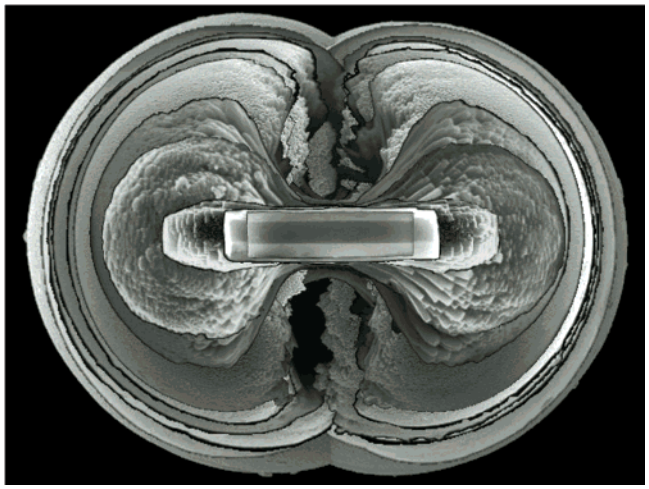

Figure 8. Successive development stages of the morphogenesis of a fluorapatite−gelatine composite visualized as a superposition. For clarity the image of each stage is surrounded by a black line. (a) Hexagonal seed, (b) dumbbell, and (c) closed sphere.[91] The size of the sphere corresponds to 100 μm.

Development and Morphogenesis of Fluorapatite Composite Structures

Within the gel that contains gelatine, calcium, phosphate, and fluoride ions, composite aggregates form within a few days. They are arranged in so-called Liesegang bands[84] and the first precipitation zone is located at the gel−liquid border with further bands forming within the gel. The aggregates continue to grow over a period of weeks. Particles located in a band lying near the phosphate solution show a specific growth mechanism (see below). For an optimal investigation of the small crystal aggreates, the gelatine is removed from the central part of the U-tube and is subdivided into the various bands. Repeated washing with hot water removes adherent gelatine from the particles and cleaned in this manner they can be investigated with scanning electron microscopical techniques (SEM). Observation of particles belonging to the same region of the gel but being different with regard to the time they remained in the diffusion chamber before they were washed out evidences a special growth mechanism. The formation of new seed crystals occurs randomly within the first weeks, and thus, there is always a mixture of different growth stages present in the gel. In principle, the morphogenesis starts with elongated hexagonal prismatic seeds with a perfect hexagonal habit. The sizes depend on the conditions of the reaction and are observed to reach maximum values of $30 \times 5 \times 5$ μm.[20] Progressive stages of self-assembled needle-shaped prisms at both ends of the seed lead to dumbbell-shaped aggregates, which complete their morphology by successive and self-similar upgrowth processes that finally result in equatorially notched spheres. Typical development stages are visualized in a superposition (see Figure 8) to give an impression of the observed growth. After the spheres are closed, a second, radial growth proceeds the mineralization, which leads to spheres with a maximum diameter of ≈1 mm.[20]

Summing up, by static diffusion of buffered calcium and mixed phosphate/fluoride solutions in an acidified gelatine gel, it is possible to observe the transformation

of special morphologies (hexagonal prisms) into completely different shapes (spheres). This growth process is obviously controlled by means of diffusion and self-organization only.

The described morphogenesis of fractal structures has not been evidenced for other composite systems, although the observed final morphologies are not restricted to the apatite−gelatine composites. In some cases spherical and dumbbell-shaped apatite particles were obtained in experiments similar to those described before but using a polyglycolide matrix instead of gelatine.[74] However, in these experiments it cannot be ruled out that a spherical or dumbbell-like prearrangement was already formed by the organic matrix before the mineralization started, especially because related systems such as polymerized formaldehyde show similar structures.[81] Dumbbell-shaped particles of barium sulfate[85] and calcium carbonate[86] were obtained by immediate precipitation using a block copolymer as an additive, but the aggregates did not show fractal structures. Summing up, the dumbbell as well as the spherical morphology of aggregates is often observed when organic molecules are present. However, dumbbell-shaped species were also obtained by the preparation of hematite by a sol−gel process in the presence of sulfate ions.[87] For the latter it was shown that the adsorption of sulfate ions varies with the orientation of the crystal faces relative to the long axis of the seed.[88] This is expected to lead to a retarded growth of the respective crystal planes and is therefore directly connected to the development of peanut-shaped particles. A similar mechanism is proposed for the microwave-induced formation of peanut-shaped calcite crystals in the presence of citrate.[89]

Fractal Growth Mechanism and Simulation

Analyzing various SEM images of different growth stages supports the interpretation that the morphogenesis of fluorapatite−gelatine composites is influenced by at least two noncrystallographic parameters: The first one is that the special morphology is the result of an upgrowth of preceding generations. The particles of successive generations are arranged in a way that the angle between their long axes and the prism axis of the mother individuum does not exceed 45° ± 5°. Second, subsequent generations of aggregates scale down by a factor of about 0.7. Following these two rules, the spheres should close after the 10th generation and the diameter of the surface crystallites is expected to be about 50 nm when the diameter of the seed is ≈4 μm. The experimental findings are in excellent agreement with the predictions from the presented model.

On the basis of these rules, calculations can be performed based on a model that was developed by using techniques of fractal geometry.[90] The resulting simulation reflects important structural details of the aggregates. Figure 9 shows an image of a two-dimensional model simulating the structure of a just closed sphere.[91] As a simplification, a 4-fold splitting for each generation is assumed, although the order of noncrystallographic splitting is certainly higher. The maximum opening angle is chosen to be 48°; the scale-down factor of each generation corresponds to 0.7. Crossing of

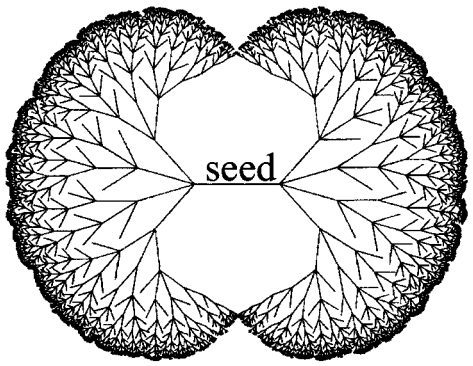

Figure 9. Image of a simulation using a two-dimensional model for the crystal growth of the fluorapatite−gelatine composites (see text for explanation). The model reproduces key features of the morphology of the aggregate, e.g., the equatorial constriction and the drop-shaped transverse section through the cavity around the seed.[91]

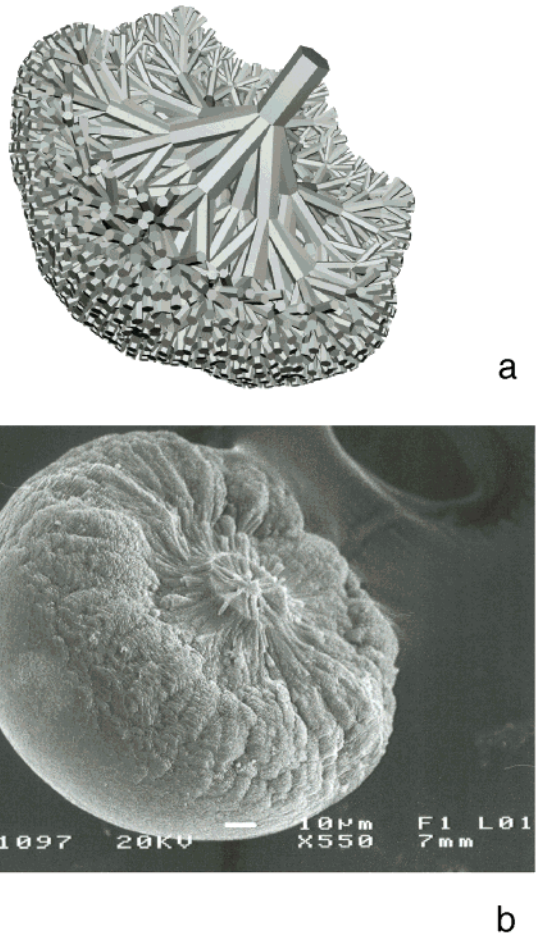

Figure 10. (a) Computer simulation of the growth of the fluorapatite−gelatine composite using a model that is based upon methods of fractal geometry using simplifying assumptions about the particle growth (see text). The morphology of the simulated aggregate reproduces (b) the structure of the synthesized spheres almost perfectly. To show more details of the calculated and the synthesized particles, the spheres have been cleft perpendicular to the seed axis.[20] Scale bar corresponds to 10 μm.

individuals is suppressed and the diffusion inhibition inside the growing dumbbell is taken into account by removing individuals growing up with an angle greater than 160° relative to the long axis of the seed. The model reflects the equatorial constriction as well as the drop-

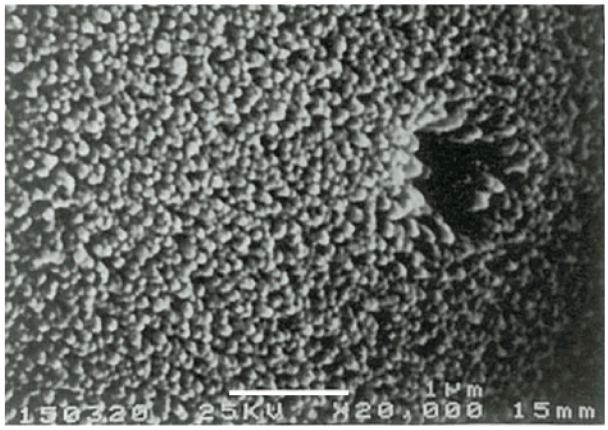

a

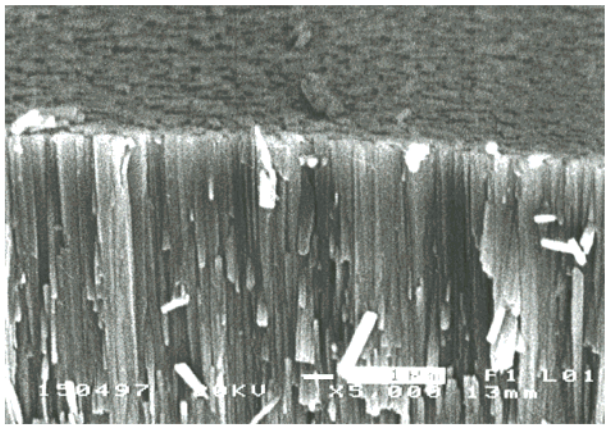

b

Figure 11. (a) Surface images of a synthesized fluorapatite−gelatine composite sphere. (b) The arrangement of the elongated particles in the outer shell of the spheroids that originate from the second growth mechanism in the biomimetic synthesis (see text) are almost parallel and bear a close resemblance to the arrangement of elongated prism bundles in enamel.[91] Scale bars correspond to 1 μm.

shaped transverse section through the cavity around the seed. A more precise three-dimensional model of a broken dumbbell in comparison with a SEM image of a broken sphere is given in Figure 10 to clarify the resemblance of the calculated and observed structures.[91]

Relations between the Self-organized Aggregates and Enamel

The similarities of the aggregates and the enamel structure becomes evident when the surface layer of a sphere (see Figure 11a) is compared to enamel prisms. The elongated crystals that are the product of the second growth mechanism in the biomimetic composites are almost parallel, and thus, they closely resemble the arrangement of elongated prism bundles in enamel (see Figure 11b). Moreover, the crystal diameter is approximately the same for enamel (26 × 68 nm[67]) and the in vitro grown composite (50−100-nm diameter). The similarity of the white but shiny colors of both materials is attributed to the resemblance of particle sizes.

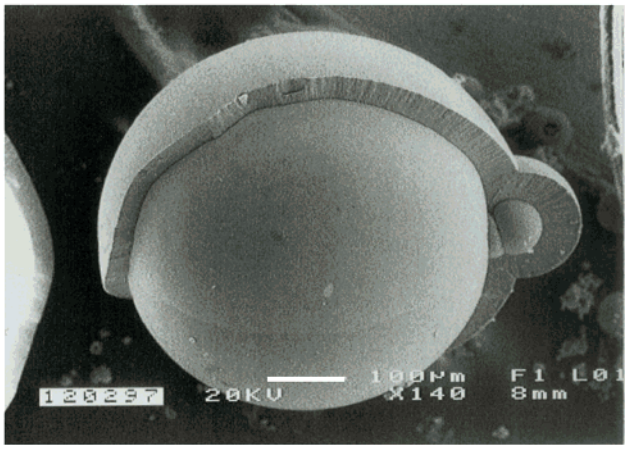

Figure 12. Image of a sphere after the second growth mechanism is finished. The outer layer has been partly removed mechanically to visualize the core−shell assembly of the aggregate.[91] Scale bar corresponds to 100 μm.

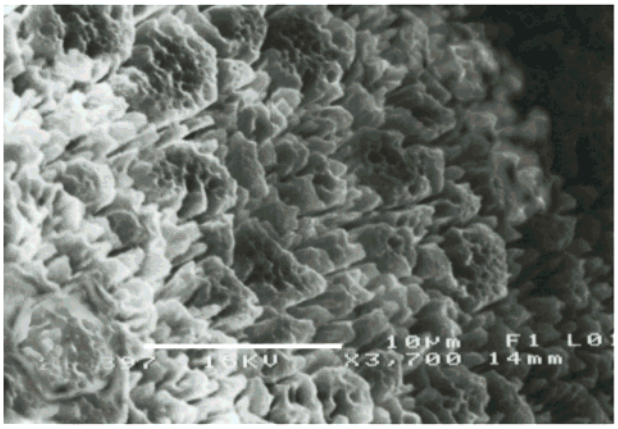

Figure 13. Surface of a fluorapatite−gelatine aggregate in the stage of a hollow sphere after EDTA attack. The surface is softened because of partial dissolution of apatite. Analogous to dental caries, the solvent reaches the interior of the spheres through these channels.[20] Scale bar corresponds to 10 μm.

The core−shell assembly (see Figure 12) consisting of the fractal core and the radial arrangement of crystals of the second growth mechanism resembles the complex organization of teeth. Although fractal structures have not been observed in natural biominerals, the analogy of the self-organized aggregates to the structure of human teeth is that we observe in both systems adjacent areas with more or less parallel arranged crystals and an underlying core that shows a more complicated organization. Thus, it is not surprising that the dissolution behavior of the self-organized aggregates shows remarkable similarities to that of enamel. This observation is especially important with respect to lesions caused by caries. Concerning chemical composition, the fractal material closely resembles enamel because it consists of about 95 wt % apatite, ≈2 wt % of the organic component and 3 wt % of water.[92]

Dissolution Behavior of the Inorganic Component of the Aggregates

The composite character as well as the relevance of the aggregates as a model material for enamel can be demonstrated by dissolving the fluorapatite in complex-forming agents such as neutral EDTA solution. It was

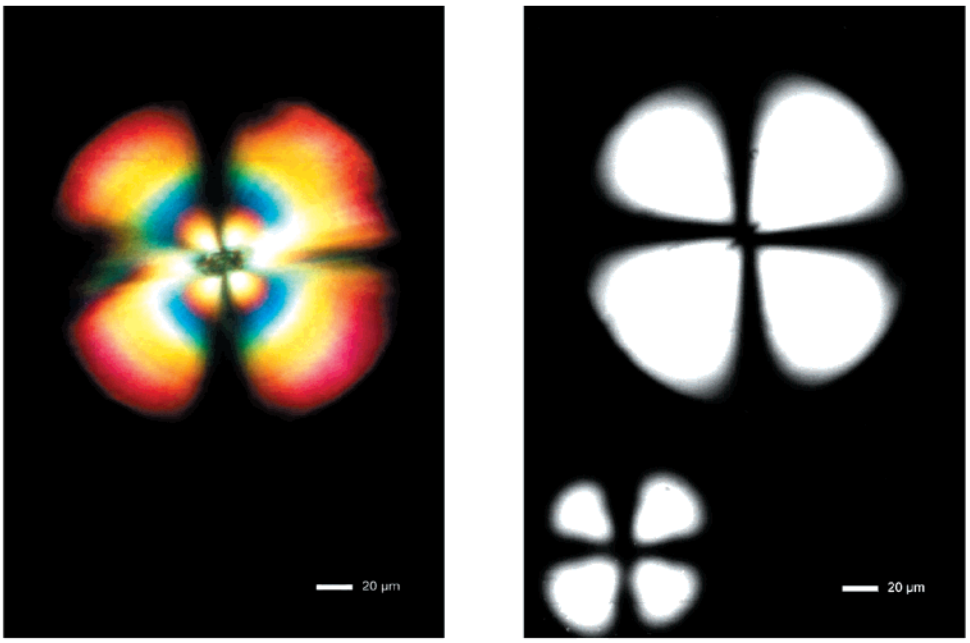

Figure 14. Light microscopic image of a typical (a) synthesized fluorapatite−gelatine composite sphere and (b) a completely decalcified gelatine residue of 125-μm diameter using a polarization microscope (crossed polarizers).[20] Scale bars correspond to 20 μm.

shown that the effect of EDTA on enamel is similar to weak acids[93] as its corrosive effects on extracted teeth produced caries-like lesions. In the case of spherocrystals, the dissolution is rather similar: First, the spheres lose their opalescence and turn pale white. This process corresponds to the formation of white spots in enamel[19] and the reason for this behavior is the development of small channels in the apatite surface that is accompanied by an alteration of the optical behavior and a "softening" of the material. The dissolution of the fluorapatite spherocrystals proceeds via different stages of hollow spheres and corresponds to the undermining activity of caries attacks. Figure 13 shows a typical SEM image of the surface of a hollow sphere illustrating the "softening" of the material. Finally, the complete sphere is dissolved and an exact copy of the original morphology remains in the form of the gelatine residue. These gelatine residues show basically the same anisotropic optical behavior (Brewster cross) as primary composites (see Figure 14), with the only difference being the lack of interference colors in the case of the gelatine sphere due to the loss of the inorganic material. As a conclusion, the observation of similar optical properties is taken as an indication that there is an interdependence of the orientation of apatite particles and the alignment of polypeptide molecules in the composite.

Possible Reasons for the Development of Fractal Structures

The optical isotropy of gelatine gels indicates that there is no macroscopic ordering before the diffusion starts. Thus, the aggregates do not represent the result of a mineralization of a preformed matrix. In contrast, during diffusion, nucleation, and mineralization a continuous interplay between gelatine molecules and the forming apatite takes place and the fractal structures are a result of a mutual interaction of the participating components. Just as it is assumed for the enamel formation, the ionotropy of gelatine leads to a reorientation of molecules due to the diffusion of inorganic ions. The inorganic and organic components interact because gelatine offers nucleation sites for the mineralization and the growing mineral particles change the orientation of neighboring polypeptides. In this context, the role of electric fields upon aggregate growth has to be clarified. The polarity of collagen and the structural properties of apatite, crystallizing either in a centrosymmetric or an acentric space group dependent on which ions are located in the channels of the crystal structure,[42] support the idea that the particle growth might be influenced by local electrical fields. Moreover, the arrangements of crystals in the fractal aggregates show a remarkable coincidence with the orientation of electrical field lines around a permanent dipole.[91] We would like to note here that bones as well as dentine show a piezoelectric and pyroelectric effect due to their polar components,[94−97] and the piezoelectric effect becomes stronger with increasing amounts of the organic component.[98] However, there is no experimental evidence for a strong permanent intrinsic electric field of the fractal aggregates as the claim of pyroelectric behavior has not been experimentally established until today.[91]

Concluding Remarks

The "*chemistry of form*"[99] is one of the most challenging fields in materials science and inorganic chemistry. In biological systems with complex compositions, a variety of different organic molecules is involved in the different steps of the morphogenesis. Their functions in

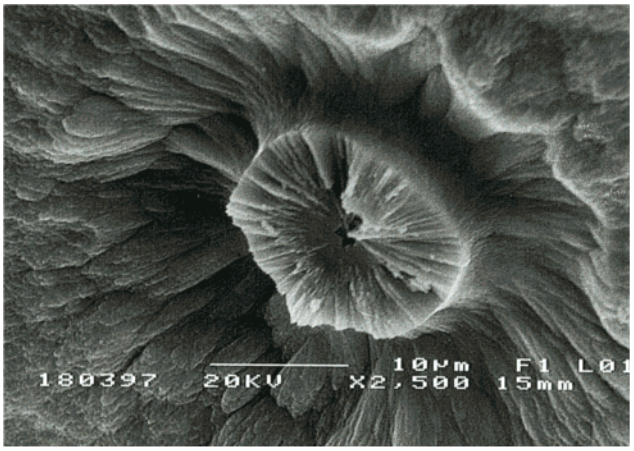

Figure 15. SEM image showing the central region of a spherocrystal that has been cleft perpendicular to the long axis of the seed to visualize the typical radiating pattern of the cross section of the seed, which is taken as an indication of the nanocomposite character of the aggregates.[100] Scale bar corresponds to 10 μm.

the course of the formation of biominerals can include the formation of precursors, the development of seeds (nucleation), and a stabilization of the growing mineral phase. Interaction of the organic molecules with the growing surface of the inorganic component induces specific changes of the crystal growth rate and, thus, of particle size and morphology. Models have been proposed to develop a picture of the mechanisms that are involved when an organic component controls the growth in its ultrastructural regions and organizes hierarchically arranged structures such as enamel prisms. It is expected that parallel to further experimental investigations of the interactions between organic and inorganic components, theoretical modeling will be of increasing importance in the development of a clear picture on an atomic scale. In this context, questions upon the composite character of biominerals and biomimetically grown aggregates will stay in the focus of interest. As shown in Figure 15, a cross section of the hexagonal seed perpendicular to the long axis, realized by bisectioning of a just closed sphere along the equatorial constriction, exhibits an unusual radial pattern that does not correspond to the cleavage properties of abiogen apatite and, thus, is attributed to be the result of the special nanocomposite situation in the seed. We assume that in accordance with the rules of self-similarity the hexagonal shape of the seed is the result of a periodic orientation of hexagonal nanoapatite crystals and that this arrangement corresponds to the organization of enamel prisms[100] in human teeth.

The formation of fractal structures in our model system strongly supports the idea that specific interactions of the organic and the inorganic component stabilize aggregates with unusually high surface areas. The use of relatively simple systems such as fluorapatite−gelatine justifies expectations to gain a deeper understanding of self-organization in organic−inorganic composite systems that are not affected by cell activities. Moreover, the remarkable structural similarities of the composite aggregates and teeth enamel open a new field for basic research activities that aim to study the possibility of reconstructing human teeth by induced remineralization.

Acknowledgment. We thank Prof. Dr. R. J. Radlanski, Berlin, for valuable discussions. Experimental support of K. Zimmermann and J. Buder is gratefully acknowledged.

References

(1) Kraus, B. S.; Jordan, R. E.; Abrams, L. *A Study of the Masticatory System−Dental Anatomy and Occlusion*; Williams & Williams: Baltimore, 1969.
(2) Schumacher, G.-H.; Schmidt, H.; Börnig, H.; Richter, W. *Anatomie und Biochemie der Zähne*; VEB Verlag Volk und Gesundheit: Berlin, 1990.
(3) Harzer, W. R. Zur Genetik der Struktur, Form, Grösse und Zahl der Menschlichen Zähne. In *Die Evolution der Zähne*; Alt, K. W., Türp, J. C., Eds.; Quintessenz Verlags-GmbH: Berlin, 1997.
(4) Weidmann, S. M.; Weatherall, J. A.; Hamm, S. M. *Arch. Oral Biol.* **1967**, *12*, 85.
(5) Höhling, H. J. *Die Bauelemente von Zahnschmelz und Dentin aus Morphologischer, Chemischer und Struktureller Hinsicht*; Hanser: München, 1966.
(6) Goldberg, M.; Carreau, J. P.; Arends, J. *Arch. Oral Biol.* **1987**, *32*, 765.
(7) Edgar, W. M.; Mullane, D. M. *Saliva and Dental Health*: British Dental Journal: London, 1990.
(8) Radlanski, R. J.; Seidl, W.; Steding, G.; Jäger, A. *Anat. Anz. Jena* **1990**, *170*, 329.
(9) Butler, W. T. *Eur. J. Oral Sci.* **1998**, *106*, 204.
(10) Schroeder, H. E. *Orale Strukturbiologie*; Thieme: New York, 1990.
(11) Skaleric, U.; Ceve, P.; Gaspirc, B.; Schara, M. *Eur. J. Oral Sci.* **1998**, *106* (suppl 1), 365.
(12) Hammer, J.; Reed, O. M.; Stanley, H. R. *J. Am. Dent. Assoc.* **1970**, *81*, 662.
(13) Soemmering, S. Th. *De Corporis Humani Fabrica. Tome 1: de Ossibus*; Varrentrapp et W.: Frankfurt/Main, 1794.
(14) Lehner, J.; Plenk, H. Die Zähne. In *W. v. Möllendorfs Handbuch der Mikroskopischen Anatomie des Menschen. Band 5*; Springer: Berlin, 1936.
(15) Tonge, C. H. Morphogenesis and Development of Teeth. In *Scientific Foundations of Dentistry*; Cohen, B., Kramer, I. R. H., Eds.; Heinemann Books: London, 1976.
(16) Steding, G. *Acta Anat.* **1969**, *68*, 37.
(17) Höhling, H. J. Special Aspects of Biomineralization of Dental Tissues. In *Handbook of Microscopic Anatomy V/6: Teeth*; Oksche, A., Vollrath, L., Eds.; Springer: Berlin, 1989.
(18) Martin, L. B.; Boyde, A.; Grine, F. E. *Scanning Microsc.* **1988**, *2* (3), 1503.
(19) Schwenzer, N. *Konservierende Zahnheilkunde*; Thieme: Stuttgart, 1988.
(20) Busch, S. Ph. D. Thesis, University of Technology, Darmstadt, 1998.
(21) Radlanski, R. J. Mikromorphologie der Menschlichen Zähne and Die Zahnentwicklung des Menschen. In *Die Evolution der Zähne*; Alt, K. W. , Türp, J. C., Eds.; Quintessenz Verlags-GmbH: Berlin, 1997.
(22) Boyde, A. Enamel. In *Handbook of Microscopic Anatomy V/6: Teeth*; Oksche, A., Vollrath, L., Eds.; Springer: Berlin, 1989.
(23) Kirkham, J.; Brookes, S. J.; Shore, R. C.; Bonass, W. A.; Smith, D. A.; Wallwork, M. L.; Robinson, C. *Connect. Tissue Res.* **1998**, *39*, 91.
(24) Lowenstam, H. A.; Weiner, S. *On Biomineralization*; Oxford University Press: Oxford, 1989.
(25) Wen, H. B.; Moradian-Oldak, J.; Leung, W.; Bringas, P., Jr.; Fincham, A. G. *J. Struct. Biol.* **1999**, *126*, 42.
(26) Uchida, T.; Tanabe, T.; Fukae, M.; Shimizu, M.; Yamada, M.; Miakel, K.; Kobayashi, S. *Histochemistry* **1991**, *96*, 129.
(27) Iijima, M.; Moriwaki, Y.; Takagi, T.; Moradian-Oldak, J. *J. Cryst. Growth* **2001**, *222*, 615.
(28) Tohda, H.; Yamada, M.; Yamaguchi, Y.; Yanagisawa, T. *J. Electron Microsc.* **1997**, *46*, 97.
(29) Aoba, T.; Komatsu, H.; Shimazu, Y.; Yagishita, H.; Taya, Y. *Connect. Tissue Res.* **1998**, *39*, 129.
(30) Felszeghy, S.; Hollo, K.; Modis, L.; Lammi, M. J. *Acta Odontol. Scand.* **2000**, *58*, 171.
(31) Chen, Q.; Linsenmayer, C.; Gu, H. H.; Schmid, T. M.; Linsenmayer, T. F. *J. Cell Biol.* **1992**, *117*, 687.
(32) Reyniers, J. A.; Trexler, P. C.; Wagner, M.; Gordon, H. A.; Luckey, T. D. *J. Dent. Res.* **1954**, *33*, 147.
(33) Orland, F. J.; Blayney, J. R.; Harrison, R. W.; Reyniers, J. A.; Trexler, P. C.; Ervin, R. F.; Wagner, M. *J. Am. Dent. Assoc.* **1955**, *50*, 259.
(34) Daculsi, G.; Kerbel, B.; Kerebel, L. M. *Caries Res.* **1979**, *13*, 277.
(35) Langdon, D. J.; Elliot, J. C.; Fearnhead, R. W. *Caries Res.* **1980**, *14*, 359.
(36) Kay, M. I.; Young, R. A.; Posner, A. S. *Nature* **1964**, *204*, 1050.

(37) Elliott, J. C.; Mackie, P. E.; Young, R. A. *Science* **1973**, *180*, 1055.
(38) Ikoma, T.; Yamazaki, A.; Nakamura, S.; Akao, M. *J. Solid State Chem.* **1999**, *144*, 272.
(39) Posner, A. S.; Diorio, A. F. *Acta Crystallogr.* **1958**, *11*, 308.
(40) Sudarsanan, K.; Young, R. A. *Acta Crystallogr. B* **1969**, *25*, 1534.
(41) Mackie, P. E.; Elliott, J. C.; Young, R. A. *Acta Crystallogr. B* **1972**, *28*, 1840.
(42) Bauer, M.; Klee, W. E. *Z. Kristallogr.* **1993**, *206*, 15.
(43) Young, R. A.; Elliott, J. C. *Arch. Oral Biol.* **1966**, *11*, 699.
(44) Hughes, J. M.; Cameron, M.; Crowley, K. D. *Am. Mineral.* **1989**, *74*, 870.
(45) Young, R. A.; van der Lugt, W.; Elliott, J. C. *Nature* **1969**, *223*, 729.
(46) van der Lugt, W.; Knottnerus, D. I. M.; Perdok, W. G. *Acta Crystallogr. B* **1971**, *27*, 1509.
(47) Braun, M.; Jana, C. *Chem. Phys. Lett.* **1995**, *254*, 19.
(48) Young, R. A. *Clin. Orthop.* **1975**, *113*, 249.
(49) Arends, J.; Davidson, C. L. *Calcif. Tissue Res.* **1975**, *18*, 65.
(50) Elliot, J. C. *Calcif. Tissue Res.* **1969**, *3*, 293.
(51) LeGeros, R. Z. *Arch. Oral Biol.* **1974**, *20*, 63.
(52) Moreno, E. C.; Kresak, M.; Zahradnik, R. T. *Nature* **1974**, *247*, 64.
(53) Munksgaard, E. C.; Bruun, C. *Arch. Oral Biol.* **1974**, *18*, 735.
(54) Frazier, P. D.; Little, M. F.; Casciani, F. S. *Arch. Oral Biol.* **1967**, *12*, 35.
(55) Mann, S.; Webb, J.; Williams, R. J. P. *Biomineralization*; VCH Verlagsgesellschaft: Weinheim, 1989.
(56) Brecevic, L.; Sendijarevic, A.; Furedi-Milhofer, H. *Colloids Surf.* **1984**, *11*, 55.
(57) Meyer, J. L. *Arch. Biochem. Biophys.* **1984**, *231*, 1.
(58) Hunter, G. K. *Connect. Tissue Res.* **1987**, *16*, 111.
(59) Jahnen-Dechent, W.; Nielsen, H.; Moos, T.; Fink. E.; Nawratil, P.; Muller-Esterl, W.; Mollgard, K. *Anat. Embryol.* **1998**, *197*, 125.
(60) Sasaki, T.; Garant, P. R. *Calcif. Tissue Int.* **1986**, *39*, 86.
(61) Shapiro, I. M.; Boyde, A. *Metab. Bone Dis. Relat. Res.* **1984**, *5*, 317.
(62) Thiele, H.; Andersen, G. *Kolloid-Z.* **1955**, *140*, 76.
(63) Thiele, H. *Protoplasma* **1964**, *58*, 318.
(64) Höhling, H. J.; Krefting, E. R.; Barckaus, R. *J. Dent. Res.* **1982**, *61*, 1496.
(65) Daculsi, G.; Kerbel, B. *J. Ultrastruct. Res.* **1978**, *65*, 163.
(66) Weiss, M. P.; Voegel, J. C.; Frank, R. M. *J. Ultrastruct. Res.* **1981**, *76*, 286.
(67) Daculsi, G.; Menanteau, J.; Kerebel, L. M. *Calcif. Tissue Int.* **1984**, *36*, 550.
(68) Mei Li, K.; Wong, W.; Mann, S. *Chem. Mater.* **1999**, *11*, 23.
(69) Heuer, H.; Fink, D. J.; Laraia, V. J.; Arias, J. L.; Calvert, P. D.; Kendal, K.; Messing, G. L.; Blackwell, J.; Rieke, P. C.; Thompson, D. H.; Wheeler, A. P.; Veis, A.; Caplan, A. I. *Science* **1992**, *255*, 1098.
(70) Walsh, D.; Mann, S. *Nature* **1995**, *377*, 320.
(71) Walsh, D.; Mann, S. *Adv. Mater.* **1997**, *9*, 658.
(72) Litvin, A. L.; Valiyaveettil, S.; Kaplan, D. L.; Mann, S. *Adv. Mater.* **1997**, *9*, 124.
(73) Göltner, C.; Cölfen, H.; Antonietti, M. *Chemie in Unserer Zeit*, **1999**, *4*, 200.
(74) Schwarz, K.; Epple, M. *Chem. Eur. J.* **1998**, *4*, 1898.
(75) Bradt, J. H.; Mertig, M.; Teresiak, A.; Pompe, W. *Chem. Mater.* **1999**, *11*, 2694.
(76) Paschalakis, P.; Vynios, D. H.; Tsiganos, C. P.; Dalas, E.; Maniatis, C.; Koutsoukos, P. G. *Biochim. Biophys. Acta* **1993**, *1158*, 129.
(77) Berman, A.; Addadi, L.; Weiner, S. *Nature* **1988**, *331*, 546.
(78) Iijima, M. *J Cryst. Growth* **1992**, *116*, 319.
(79) Iijima, M.; Moriwaki, Y. *J. Cryst. Growth* **1989**, *96*, 59.
(80) Kniep, R.; Busch, S. *Angew. Chem.* **1996,** *35*, 2624.
(81) Wunderlich, B. Spheroliths. In *Macromolecular Physics*; Academic Press: New York, 1973.
(82) Armington, A. F.; O'Connor, J. J. *Mater. Res. Bull.* **1969**, *3*, 923.
(83) Kerebel, B.; Daculsi, G.; Verbaere, A. *J. Ultrastruct. Res.* **1976**, *57*, 266.
(84) Henisch, H. K. *Crystals in Gels and Liesegang Rings*; Cambridge University Press: Cambridge, 1988.
(85) Qi, L.; Cölfen, H.; Antonietti, M. *Angew. Chem., Int. Ed.* **2000**, *39*, 604.
(86) Cölfen, H.; Qi, L. *Chem. Eur. J.* **2001**, *7* (1), 116.
(87) Sugimoto, T.; Kahn, M. M.; Muramatsu, A. *Colloids Surf.* **1993**, *A70*, 167.
(88) Sugimoto, T.; Wang, Y. *J Colloid Int. Sci.* **1998**, *207*, 137.
(89) Clemente, M. *J. Cryst. Growth* **1996**, *169*, 339.
(90) Mandelbrot, B. B. *Die Fraktale Geometrie der Natur*; Mandelbrot, B. B. , Ed.; Birkenhäuser: Basel, 1991.
(91) Busch, S.; Dolhaine, H.; DuChesne, A.; Heinz, S.; Hochrein, O.; Laeri, F.; Podebrad, O.; Fietze, U.; Weiland, T.; Kniep, R. *Eur. J. Inorg. Chem.* **1999**, *10*, 1643.
(92) Okazaki, M.; Tokahashi, J.; Kimura, H. *J. Osaka Univ. Dent. Sch.* **1989**, *29*, 47.
(93) Schatz, A.; Martin, J. J. *Bl. Zahnheilkunde* **1965**, *26*, 191.
(94) Andrew, C.; Bassett, L. *Calcif. Tissue Res.* **1968**, *1*, 252.
(95) Fukada, E.; Yasuda, I. *J. Phys. Soc. Jpn.* **1957**, *12*, 1158.
(96) Cochran, G. V. B.; Pawluk, R. J.; Bassett, C. A. L. *Arch. Oral Biol.* **1967**, *12*, 917.
(97) Lang, B. L. *Nature* **1966**, *12*, 704.
(98) Ogolnik, R.; Kleinfinder, A.; Fremaux, A.; Geiger, D. *J. Biol. Buccale* **1976**, *4*, 117.
(99) Mann, S. *Angew. Chem., Int. Ed.* **2000**, *39*, 3392.
(100) Busch, S.; Schwarz, U.; Kniep, R., in preparation.

CM0110728